submitted to the Astrophysical Journal

Evidence for Multiple Companions to Upsilon Andromedae [1]

R. Paul Butler[2], Geoffrey W. Marcy[3], Debra A. Fischer[3], Timothy W. Brown[4], Adam R. Contos[5], Sylvain G. Korzennik[5], Peter Nisenson[5], Robert W. Noyes[5]

ABSTRACT

The bright F8 V star υ Andromedae was previously reported to have a 4.6 day Doppler velocity periodicity, consistent with a Jupiter–mass companion orbiting at 0.059 AU. Follow–up observations by both the Lick and AFOE planet survey programs confirm this periodicity, and reveal additional periodicities at 242 and 1269 days. These periodicities are consistent with Keplerian orbital motion, and imply two additional companions orbiting at 0.83 and 2.5 AU, with minimum ($M \sin i$) masses of 2.0 and 4.1 Jupiter-masses respectively.

Non–Keplerian explanations for the observed Doppler velocity variations are examined, including radial and nonradial pulsations, rotational modulation of surface features, and stellar magnetic cycles. These explanations seem unlikely based on the observed photometric and chromospheric stability of the star.

This putative three planet system is found to be dynamically stable by both analytic techniques and numerical simulations. The outer two companions both reside in eccentric orbits, as do all 9 known extrasolar planet candidates in distant orbits. If real, this multiple–planet system is the first around a main-sequence star, and its study should offer insights into planet formation, planet–planet interactions, and the observed eccentricities of planetary orbits.

Subject headings: stars: planetary systems, stars: individual (HD 9826)

---

[1]Based on observations obtained at Lick Observatory, operated by the University of California, and at the Whipple Observatory, operated by the Smithsonian Astrophysical Observatory.

[2]Anglo–Australian Observatory, PO Box 296, Epping, NSW Australia 1710

[3]Department of Physics and Astronomy, San Francisco State University, San Francisco CA, USA 94132 and at Department of Astronomy, University of California, Berkeley, CA USA 94720

[4]High Altitude Observatory, National Center for Atmospheric Research, P.O. Box 3000, Boulder, CO USA 80307

[5]Harvard–Smithsonian Center for Astrophysics, Cambridge, MA USA 02138

1. Introduction

All $\sim$20 extrasolar planets discovered over the last four years have been revealed by precision Doppler velocity surveys (Mayor et al. 1998; Marcy & Butler 1998; Noyes et al. 1997; Cochran et al. 1997). It is not surprising that these discoveries have all been of single planet systems. While a minimum of seven Doppler velocity measurements are needed to describe the orbit of a single planet, in practice 20 observations spread over more than one orbital period are typically required to reliably determine orbital parameters. The discovery of a system with two or more planets by the precision Doppler technique requires a time span longer than the orbital period of the most distant planet, and many dozens of observations.

The extrasolar planets found to date have been surprising in two respects. About half of these planets have been found orbiting inside 0.2 AU. The extreme temperatures and small amount of protostellar material in these regions suggest that these planets formed further out in their respective protoplanetary disks, and then migrated in to their current positions.

All nine of the remaining planets, orbiting between 0.2 and 3 AU, have significantly non–zero orbital eccentricities ($e > 0.1$). Planets formed in a dissipative viscous disk are expected to have circular orbits at the time the disk evaporates. Most pre–1996 theories of planet formation posited that extrasolar planets would be in circular orbits similar to the architecture of the Solar System (Boss 1995; Lissauer 1995).

Two classes of theories have been advanced to explain the small–orbit "51 Peg-type" planets. Orbital migration driven by tidal interactions with the protoplanetary disk (Goldreich & Tremaine 1980; Lin & Papaloizou 1986) can bring a Jupiter–mass planet to within 0.05 AU. The planet can then be stabilized against further orbital degradation until the disk evaporates by a number of mechanisms (Lin et al. 1996; Ward 1997; Trilling et al. 1998). Alternatively, Rasio & Ford (1996) have suggested that gravitational encounters between planets in a post–disk environment could result in a planet being flung into an orbit with a very small periastron distance. Tidal interactions by the host star could then circularize the orbit with a separation of a few stellar radii. A number of theories have been suggested to explain the eccentric planets, including gravitational interactions between planets (Weidenschilling & Marzari 1996; Rasio & Ford 1996; Levison et al. 1998), gravitational interactions with a companion star or a passing star (Holman et al. 1997; Mazeh et al. 1997; de la Fuente Marcos & de la Fuente Marcos 1997; Laughlin & Adams 1998), and tidal interactions between the protoplanet and the disk (Artymowicz 1993).

If planet-planet interactions are the dominant source of orbital evolution within planetary systems, additional companion planets should ultimately be detected in most of the currently known planetary systems. If planet-disk interactions are primarily responsible for sculpting planetary systems, then systems of multiple Jupiter–mass planets might be relatively rare, or additional companions in these systems might orbit further than 10 AU from the host star, making them difficult to detect with current technology.

This paper reports the Doppler velocity measurements of the bright F8V star υ Andromedae. This star has previously been reported to have a "51 Peg–like" planet with a 4.6 day orbit (Butler et al. 1997). In addition, the original discovery paper noted "evidence for variability in the gamma velocity" of the 4.6 day periodicity with a "timescale of about 2 yr". Subsequent observations reported here confirm this variation, and suggest that the residual Doppler velocities are Keplerian in nature. The stellar characteristics of υ Andromedae are reported in section 2. The precision Doppler measurements and possible Keplerian orbital solutions are considered in the third section. Section 4 presents alternative explanations for the observed Doppler velocity variations. A discussion follows.

2. Stellar Characteristics

υ Andromedae (HD 9826, HR 458, HIP 7513) is probably a single star. The Bright Star Catalog (Hoffleit 1982) lists it as a spectroscopic binary with an amplitude of 1.8 km s^{-1} and a period of 198 days. This result is inconsistent with the ten year survey of Duquennoy & Mayor (1991) who found that the Doppler velocity of υ Andromedae is constant to within their measurement uncertainty of 360 m s^{-1}, in agreement with Morbey & Griffin (1987) and the precision velocity study of Butler et al. (1997). Two optical companions are almost certainly not physically associated as they have unrelated proper motions.

2.1. Hipparcos

Hipparcos made 93 observations of υ Andromedae. The Hipparcos magnitude, $M_{\rm HIP}$, is 4.212, with a scatter of 0.006 magnitudes, consistent with measurement uncertainties. Transforming $M_{\rm HIP}$ to V magnitude yields a value of 4.10. Both the Hipparcos and Bright Star catalogs assign a spectral type of F8V to υ Andromedae, consistent with $B-V$ $= 0.536$. The Hipparcos parallax of 74.25 mas corresponds to a distance of 13.47 pc (Perryman et al. 1997). The absolute V magnitude of υ Andromedae is 3.45, and the absolute luminosity is 3.0 L$_\odot$.

2.2. Stellar Modeling

Fuhrmann et al. (1998) derived the stellar characteristics of υ Andromedae from high resolution spectral synthesis, yielding $T_{\rm eff} = 6100 \pm 80$, $\log(g) = 4.0$, and $v \sin i = 9.5$ km s^{-1}, in good agreement with the results of Gonzalez (1997). Assuming a bolometric correction of -0.08, Fuhrmann et al. (1998) find the radius of υ Andromedae to be 1.69 R$_{\odot}$. Alternatively, Ford et al. (1998) assume a bolometric correction of -0.01, which yields a radius of 1.56 R$_{\odot}$.

The metallicity of υ Andromedae from Fuhrman et al. (1998), [Fe/H] = 0.09$\pm$0.03, is somewhat higher than that derived from previous studies, but similar to the result of Edvardsson et al. (1993) who also find [Fe/H] = 0.09. Gonzalez (1997) finds [Fe/H] = 0.17$\pm$0.08.

Based on the spectral classification, the mass of υ Andromedae is estimated to be 1.2 M$_{\odot}$ (Gray 1992). The mass and age of υ Andromedae derived from stellar interior modeling is 1.34 M$_{\odot}$ and 2.6 Gyr, respectively (Ford et al. 1998). In this paper, we adopt an intermediate mass of 1.3$\pm$0.1 M$_{\odot}$.

2.3. Chromospheric Diagnostics

From calibrations of the CaII H&K emission, Baliunas et al. (1997) estimate the age of υ Andromedae to be 5 Gyr, and the rotational period to be 12 days. Ford et al. (1998) point out that a 12 day rotation period and a radius of $\sim$ 1.6 R$_{\odot}$ yields an equatorial rotational velocity of $\sim$ 6.6 km s^{-1}, inconsistent with $v \sin i \sim 9$ km s^{-1}. Either the spectroscopically inferred $v \sin i$ values are too high by 3 km s^{-1} (unlikely), or the rotation period is ≤ 9 days.

Saar et al. (1998) have studied the intrinsic Doppler velocity variations, "jitter", caused by photospheric variations that were seen in the Lick precision Doppler survey of 107 main sequence stars. Based on the calibration with CaII H&K emission, it is estimated that υ Andromedae should exhibit a velocity jitter of $\sim$10 m s^{-1}.

3. Doppler Velocity Observations and Orbital Solution

3.1. Observations

Precision Doppler velocity measurements of υ Andromedae have been independently carried out by the Lick and AFOE planet search programs. Each group uses a cross–

dispersed echelle spectrometer, and an Iodine absorption cell (Marcy & Butler 1992) to provide wavelength calibration. The Lick measurements have been made with the 3–m "Shane" and 0.6–m "CAT" telescopes, both of which feed the "Hamilton" coude spectrometer (Vogt 1987). The AFOE observations have been carried out with the 1.5–m Whipple telescope, which feeds the "Advanced Fiber–Optic Echelle" (AFOE), a fiber–coupled bench–mounted spectrometer (Brown et al. 1994). The resolution of both spectrometers is about ∼50,000. Iodine provides a dense forest of absorption lines from 5000 to 6000 Å, allowing a precise determination of the wavelength and the spectrometer PSF (Butler et al. 1996).

υ Andromedae has been observed 89 times as part of the Lick Observatory planet survey program. These observations, listed in Table 1 and shown in Figure 1a, span 11.5 years. The first five observations were made between 1987 Sept and 1988 Feb. Subsequent observations began in mid 1992 and continue through to the present epoch. The "Hamilton" spectrometer was upgraded in 1994 Nov, improving resolution and wavelength coverage. Measurement uncertainties prior to 1994 Nov are 13 m s^{-1}, while subsequent observations have associated errors of 9 m s^{-1}, set by the rotational broadening of the lines and the typical S/N ratio (∼200) of the spectra. The RMS of the Lick velocities is 75 m s^{-1}, with peak–to–peak variations of 300 m s^{-1}. Observations made since 1994 November include the Ca II IR triplet, which serves as a chromospheric diagnostic, similar to the CaII H&K lines (Shirts & Marcy 1999).

The AFOE planet survey has made 52 observations of υ Andromedae, beginning in 1994 September. These observations, shown in Figure 1b and listed in Table 2, have typical measurement error of ∼13 m s^{-1}, similar to the Lick observations. The RMS and peak–to-peak variations are also similar to Lick.

3.2. Keplerian Orbital Solution

During time scales of a few months or less, the Doppler velocity signal of υ Andromedae is dominated by a 4.6 day periodicity, as shown in Figure 4 of Butler et al. (1997). On longer timescales, the gamma velocity of the 4.6 day periodicity varies by about 100 m s^{-1}, though the 4.6 day variation remains phase–locked.

Periodicities longer than 4.6 days were initally investigated by subtracting the previously detected 4.61 day Keplerian from the data shown in Figure 1a. These velocity residuals are shown in Figure 2. A 3.5 year periodicity is apparent to the eye, and was independently found by both the Lick and AFOE teams. A periodogram (Black & Scargle

1982) of the velocity residuals from Figure 2 are shown in Figure 3a. The 3.5 year periodicity dominates this periodogram. A secondary peak near 500 days is an alias, introduced by the window function.

The best–fit two Keplerian model, with orbital periods of 4.617 and 1269 days, reduces the RMS of the Lick velocities to 30 m s^{-1}, about a factor of two greater than the expected measurement uncertainties. We were thus compelled to search for additional periodicities. Figure 3b shows the residuals to the best–fit 2-Keplerian model for the Lick data, while Figure 3c shows the periodogram of these residuals. A remaining 242 day periodicity is uncovered in the periodogram which would occur by chance in less than 0.1% of random data sets.

The residuals of the Lick Observatory observations to a three Keplerian model are shown in Figure 4a. The orbital parameters of the three Keplerian orbits are listed in Table 3. The RMS of the 3 Keplerian fit is 15.1 m s^{-1}, consistent with measurement uncertainty from the combination of measurement error (9 m s^{-1}) and the expected stellar jitter (10 m s^{-1}).

Figure 4b shows the Lick velocities phased with a 4.617 day period, after first removing the 242 and 1269 day periodicities. This innermost companion, υ Andromedae "b", has a velocity semiamplitude of 74.5 m s^{-1} and an eccentricity of 0.042 (consistent with circular). The minimum mass ($M \sin i$) of the companion is 0.72 M_{JUP}, and the semimajor axis is 0.059 AU. This 4.6-day companion is clearly the same one identified by Butler et al. (1997).

The Lick residual velocities, phased with a 242 day period, are shown in Figure 4c, in which the two Keplerian curves with P=4.617 d and P=1269 d have been removed. The semiamplitude of υ Andromedae "c" is 56.0 m s^{-1} and the eccentricity is 0.23. The minimum mass ($M \sin i$) of the companion is 1.98 M_{JUP} and the semimajor axis is 0.83 AU.

The Lick residual velocities, phased with a 1269 day period, are shown in Figure 4d, after first removing the two Keplerian curves that have P=4.617 and P=242 day. The semiamplitude of υ Andromedae "d" is 69.5 m s^{-1} and the eccentricity is 0.36. The minimum mass ($M \sin i$) of the companion is 4.11 M_{JUP} and the semimajor axis is 2.50 AU.

While the formal uncertainty in the period of companion "d" is 9 d from the Monte–Carlo tests of the Lick data, we suspect that the uncertainty could be several times as much. Observation through several orbits of companion "d" will be necessary to accurately determine its period.

A periodogram of the velocity residuals (Fig 4a), obtained by removal of all three putative companions, is shown in Figure 5. The 0.1% false alarm level is indicated as a dotted line. After removing the three Keplerians, none of the remaining periodicities show significant power.

The AFOE data also show a combination of the three periods. The parameters for the best fit to the AFOE data alone are given in Column 2 of Table 3. Figure 6a shows the residuals of the AFOE velocities from that fit, with RMS value of 12.1 m s^{-1}. Figure 6 b,c, and d show the AFOE velocities phased to the same fit for each of the three periods, in each case after subtracting the Keplerian velocity curves with the other two periods (as in Figure 4 b,c, and d for the Lick data).

The fit parameters derived from the AFOE data for companions "b" and "c" are identical within errors to those derived from the Lick data, and thus give very strong evidence that these two variations are real and Keplerian. For companion "d", while the values of the amplitude, eccentricity, and ω are consistent with those derived from the Lick data, the derived period, 1481 days, is longer by an amount greater than the formal errors of the fit. However the total span of the AFOE data, 1596 days, is barely longer than this derived period, so the true uncertainty in the fit is larger than given by the formal errors.

Column 3 of Table 3 gives the best fit to the combined Lick and AFOE data sets. Figure 7a shows velocity residuals of the combined data to this fit, and Figure 7 b,c,d shows the corresponding phased residuals for each companion in turn, after subtracting the velocity fit for the other two companions. For companions "b" and "c", the orbital parameters are essentially identical to those for the independent fits. For companion "d", the period from the combined data is close to that for the Lick data alone, because it is mainly constrained by the longer span of the Lick data, 4196 days. The good fits to the Lick data alone, and to the combined data, suggest that a period near 1268 days is the most likely. However, because of the uneven sampling of the existing data there is some ambiguity in this value, which can be only be resolved by more data to adequately sample a second complete cycle.

3.3. Astrometric Constraints

Doppler velocity information is sufficient to solve for all orbital parameters except i, the orbital inclination angle. Hipparocos astrometry is able to put upper limits on the inclination angle. The amplitude of an astrometric wobble due to an orbiting companion increases linearly with increasing mass and separation of the companion. For the system proposed here, the outer "d" companion will dominate the astrometric signal. With a mass of $4.1/\sin i$ M_{JUP}, the expected astrometric signal that the "d" companion would impose on υ Andromedae is $0.56/\sin i$ milliarcseconds (mas). The quoted uncertainty in the Hipparcos parallax, based on a model that fits parallax and proper motion, is 0.72 mas. If $\sin i$ were smaller than 0.8, the astrometric wobble would have been detectable within Hipparcos measurement uncertainty. If we use a more conservative 2-sigma limit for the upper limit of the astrometric wobble, then $\sin i$ is constrained to lie between 0.4 and 1, and the maximum mass of the "d" companion is 10 M_{JUP}. Assuming that the three planets are coplanar, Hipparcos astrometry constrains the mass of each planet to be at most 2.5 times the minimum mass at the 95% confidence level. We caution that the possible scattering history of the three companions might imply non–coplanar orbits.

4. Alternative Explanations

A number of astrophysical effects can mimic Keplerian Doppler velocity variations. These include radial and nonradial pulsations, rotational modulation of surface features (i.e. spots), and long term stellar magnetic cycles. In addition, aliasing can present a serious challenge for unevenly sampled data exhibiting multiple periodicities.

4.1. Radial Pulsations

In the case of υ Andromedae, radial pulsations can immediately be ruled out as the cause of the 242 and 1269 day periodicities. A 242 day pulsation with an amplitude of 56 m s^{-1} would cause the radius of the star to change by 0.55 $R_\odot$, while the 1269 day periodicity would lead to 4.5 $R_\odot$ change. Radius variations of this order would render υ Andromedae a naked eye variable. If the 4.6 day periodicity were due to stellar pulsation, the radius would change by 0.013 $R_\odot$, which is ruled out by Hipparcos photometry, unless the surface temperature variations conspired to hide the luminosity changes.

4.2. Rotational Modulation

With a rotation period of 12 days or less, it is implausible that rotational modulation could be the cause of the 242 and 1269 day periodicities. Given the uncertainties in the determination of the rotational period, a 4.6 day period cannot be ruled out. If rotational modulation of spots were the cause of the observed Doppler velocity variations, it is expected that υ Andromedae would show a matching photometric periodicity with an amplitude of several hundredths of a magnitude. For example, the young spotted G0 V star HD 166435 exhibits Doppler variations with a 3.8–day period, a semiamplitude of $\sim$80 m s^{-1}, and a matching photometric periodicity with a semiamplitude of 0.06 magnitudes (Queloz & Henry 1998). In contrast, periodogram analysis (Black & Scargle 1982) and string length minimization codes find no significant power near 4.6 days in the Hipparcos photometry of υ Andromedae, placing a conservative upper limit of 0.01 magnitudes to any photometric variation.

4.3. Nonradial Pulsations

Gray (1997) has suggested that nonradial pulsations may mimic a Keplerian Doppler velocity signal. Gray notes, "Nonradial oscillation may not be a viable explanation for periods exceeding a few days, as such long periods are not expected, and because integration of the radial velocity curves imply unreasonably large motion of the stellar surface". Studies of line bisector variations have now ruled out nonradial pulsations as the cause of the observed Doppler velocity variations for two of the short period "51 Peg-like" cases, 51 Peg (Brown et al. 1998 a,b; Gray 1998; Hatzes et al. 1998) and τ Boo (Brown et al. 1998 a,b; Hatzes & Cochran 1998). Studies of line bisector variations in υ Andromedae are warranted.

4.4. Magnetic Cycles

Periodic variations in a stellar photosphere related to long term stellar magnetic cycles, such as the 11 year solar cycle, may mimic Doppler velocity variations (Saar & Donahue 1997). For example, variations in the number and distribution of spots, and changes in the shapes of line bisectors are both observed on the Sun. Long term magnetic cycles on the Sun and other solar type stars also show up as periodic variations in the emission of the CaII H&K line cores (Baliunas et al. 1995). Shine & Linsky (1972) showed that the core of the Ca II IR triplet line 866.2 nm brightens in solar plage, and Larson et al. (1993) have demonstrated the utility of the core as a chromospheric diagnostic, giving results similar to the H&K lines (Shirts & Marcy 1999).

If long term Doppler velocity variations are due to magnetic cycles, then it is expected that these variations will track changes in both the H&K lines and the Ca II IR triplet lines. For example, Walker et al. (1995) have simultaneously observed the Ca II IR triplet while taking precision Doppler velocity measurements of 21 stars. They found that the photometric variable κ^1 Ceti (G5 V) shows velocity excursions of up to 70 m s^{-1} which correlate with changes in the equivalent width of the 866.2 nm line. For the case of the

Sun, McMillan et al. (1993) found that the disk–integrated Doppler velocity variations were below detection limits, 4 m s^{-1}, over a 5 year period.

Saar et al. (1998) have examined the original 107 stars in the Lick Observatory planet survey for correlations between Doppler velocity variations and CaII H&K measurements. Stars with weak H&K emission ($P_{\rm rot} \geq 15$ days) showed no intrinsic velocity variations above 5 m s^{-1}, while the more rapidly rotating stars ($P_{\rm rot} < 10$ days) showed intrinsic Doppler velocity variations of 10 to 30 m s^{-1}. From the Saar et al. (1998) calibration, we estimate that υ Andromedae is subject to intrinsic velocity scatter of 10 m s^{-1}.

All of the Lick spectra taken since 1994 Nov have included the Ca II IR triplet. These chromospheric measures are taken simultaneously with the Doppler measurements as they come from the same exposures. The Iodine absorption lines that serve as a velocity metric between 5000 and 6000 Å die out above 7000 Å, leaving the IR triplet lines unblended. The chromospheric emission from υ Andromedae is measured from the "filling-in" of the core of the Ca II 866.2 nm line. We define a core bandpass 0.07 nm centered on the core and measure the flux within that bandpass for each spectrum. We define two "continuum" bandpasses, each 0.2 nm wide, centered 0.34 nm from the core, residing in the far wings of the 866.2 absorption line. Selection of these bandpasses follows the guidance of Larson et al (1993). Finally, we form the ratio of the flux per unit wavelength in the core to that in the continuum, thereby establishing a quantity similar to an equivalent width (EW) for the core. Increasing chromospheric activity in the star should produce an increase in this EW.

Figure 8a shows our measurements of the EW for the Ca II 866.2 nm core. The EW errors are typically 2% due to photon statistics in that region of the spectrum at which the CCD (for most observations) had poor sensitivity. No significant variation in the core of the Ca II line is seen. Figure 8b shows the periodogram of the those same EW measurements of the Ca II 866.2 core. None of the peaks in the periodogram is statistically significant, as verified with Monte–Carlo tests in which we scrambled the EW values but kept the observation times fixed. Thus, we find no compelling periodicity in the chromospheric emission from υ Andromedae. However, we note the existence of two peaks in the Ca periodogram (Fig 8b) that reside between periods of 200-300 d at a power of $\sim$4. This peak level is not statistically compelling. But the peaks constitute a warning to investigate further the existence of intrinsic periodicities in the photosphere with periods of 200-300 d, possibly related to the velocity periodicity seen at a similar period.

4.5. Aliasing

The uniqueness of the proposed three Keplerian orbital solution was tested with a genetic–algorithm routine which searches all parameter space. This routine found the same best–fit solution as the non–linear least squares routine used to derive the parameters listed in Table 3. No other set of parameters yield distinct solutions with fits of comparable quality.

The possibility that the "c" component, with a 242 day period, is spurious and due to the window function was tested by a Monte–Carlo simulation. Several artificial data sets were constructed by using the sum of the Doppler velocities from components "b" and "d", plus a random noise component that was different for each artificial set. The noise itself consisted of the sum of two parts, one uniformly distributed in Doppler velocity with a peak-to-peak velocity range of 110 m s^{-1}, and the other a Gaussian-distributed component with mean of zero and an RMS of 15 m s^{-1}. Together, these typically gave an RMS fit to the two Keplerian orbit of 35 m s^{-1}. The epochs for the synthetic observations were the same as for the real observations.

Fitting the resulting synthetic data sets with three Keplerians typically gave χ^2 values that were a factor of three worse (larger) than for the real data. The synthetic data set that gave the best fit was still more than a factor of two worse than the real data. The periods for "c" component in the synthetic data sets scattered all over the allowed range, with a slight preference for periods below 150 days. Periods around 250 days were certainly not preferred.

5. Discussion

The expected uncertainties in our Doppler velocity measurements for υ Andromedae consist of measurement error, $\sim$10 m s^{-1}, and intrinsic photospheric velocity jitter, $\sim$ 10 m s^{-1}, based on chromospheric activity indicators (Saar et al. 1998). When added in quadrature, these two effects cause a final uncertainty in the velocity of the center of star of 15 m s^{-1}, much less than the observed scatter of 75 m s^{-1} in the raw velocities.

Invoking only one periodicity, the residuals to a Keplerian fit have an RMS of $\sim$65 m s^{-1}, a factor of 4 larger than expected velocity uncertainties. The resulting periodogram of the residuals shows a strong peak at 3.5 years. We were initially driven to expand the model to include this additional second companion to explain the data.

Simultaneously solving for the 2 Keplerian orbits leaves residuals with an RMS of $\sim$30 m s^{-1}, about a factor of two greater than the expected scatter. However, the residuals are correlated in time and exhibit a strong periodogram peak at a remaining third periodicity. The three periodicities are not harmonics of each other and do not correspond to aliases introduced by the window function. This is true for both the fits to the Lick data and the AFOE data. None of the three periods correspond to known stellar-interior time scales (dynamical, rotation, magnetic buoyancy, spot cycle). Periodogram analysis of our chromospheric diagnostic shows no significant power near the periods found in the Doppler velocity data. Therefore, we were compelled to expand the model to include three companions. Doing so yields fits to the Lick and the AFOE data sets with RMS consistent with instrumental uncertainty plus stellar noise and χ^2 of order unity.

The possibility of three Jupiter–mass planets orbiting within 2.5 AU of each other immediately raises questions about the dynamic stability of this putative system. Using the "Hill stability" criterion, that planets are forbidden to ever make close approaches, it can be shown that this system is stable, except for extreme values of $\sin i < 0.2$. Such extreme values of $\sin i$ are ruled out by Hipparcos astrometry (see Section 3.3). However the orbital elements of the individual planets may be subject to long term perturbations (Gladman 1993). The inner planet, υ Andromedae "b", exceeds the minimum stability criterion by more than than an order of magnitude, suggesting relatively little interaction with the two outer companions. Greg Laughlin (personal communication) has carried out a numerical simulation of the system of 3 planets described in Table 3. In these simulations, certain regimes of orbital parameter space appear unstable while others appear stable. The eccentricities of the 3 orbiting bodies may vary chaotically due to gravitational interactions, and orbit crossings render some orbital parameters physically implausible. Dynamical calculations may help determine which inclinations and masses are plausible.

The eccentricity of the inner (b) companion, 0.042, is consistent with circular motion. Most of the planets orbiting within 0.1 AU are in nearly circular orbits, with the possible exception of HD 217107 (Fischer et al. 1999). This is not surprising as the tidal circularization timescale for the "51 Peg–like" planets is $\sim$1 Gyr (Rasio & Ford 1996; Marcy et al. 1997; Ford et al. 1998).

The outer two companions both have significantly non–zero eccentricity. This continues the observational trend: all of the extrasolar planets orbiting beyond 0.2 AU have eccentricity greater than 0.1. This unexpected result suggests that the theories of planetary formation and evolution must provide an explanation for these eccentricities as a common by-product. Assuming that the three companions are real, planet–planet interactions constitute a plausible explanation for the orbital evolution of this system.

Recent improvements in computer speed and computational algorithms make possible increasingly realistic simulations of evolving planetary systems. For example, Levison et al. (1998) have constructed models that begin with thousands of protoplanets embedded in a gas/dust disk. These systems evolve over several Gyrs, until orbital stability is achieved. Planet–planet interactions typically dominate in forming the final stable architecture of a given system. Many of the model systems formed in this way resemble the υ Andromedae system.

Assuming the albedo of all three companions in the υ Andromedae system are similar to Jupiter ($\sim$0.35), the equilibrium temperature for the companions, in order of increasing distance from the central star, are 1370, 365, and 210 K (Guillot et al. 1996). Internal heating probably raises the temperature of the middle (c) companion above the boiling point of water, while the the outer (d) companion is probably pushed up to near the water freezing point at a pressure of 1 atm.

The maximum angular separation of the three planets from the central star are 0.0045, 0.076 and 0.25 arc seconds. Given the extreme luminosity ratio of the central star relative to the planets, direct detection at optical wavelengths will be difficult. This ratio is improved by two to four orders of magnitude in the near IR, portending possible detection with new IR instrumentation (Burrows et al. 1998).

At a distance 13.5 pc, υ Andromedae is an ideal target for the Space Interferometry Mission (SIM). The design requirements of SIM call for 4 μas astrometric precision. The radial velocity amplitudes for each of the three planetary companions are comparable in magnitude, however, the angular displacement of the stellar photocenter that each induces is naturally quite different. Figure 9 shows the astrometric signature of υ Andromedae from the 3 planetary companions discussed in this paper. This simple model assumes an edge-on orbit, observed at evenly-spaced, 30 day intervals over 8 years. The inner companion, b, with a periodicity of 4.6 days, produces a small peak-to-peak displacement of about 8 μas that is not visible on the scale of this plot. The outer companion, d, with an orbit of 3.5 years induces the largest displacement, $\sim$1200 μas peak-to-peak. However, one complication in obtaining an astrometric orbital solution for companions in orbits that are longer than half of the mission lifetime (or half of the observation interval) is that part of the orbital displacement will be absorbed in the proper motion solution (Black & Scargle, 1982). This situation is improved with a long time baseline of high quality proper motion observations. Alternatively, the orbital period provided here by the Doppler velocity observations would eliminate the long orbit as a free parameter and SIM would effectively detect the intermediate period companion and resolve the orbital inclination. The Doppler velocity measurements also play an important role in confirming the reality of short period, low amplitude astrometric displacements (like component b) which still have strong Doppler velocity signatures.

The formation of three Jupiter–mass companions having these apparent orbital sizes and eccentricities is difficult to explain in the context of current theories of the origin of planetary systems. Most such theories suppose that gas giants form beyond a distance where water condenses into ice, typically $\sim$4 AU from the star (Boss 1995; Lissauer 1995). However all three companions around υ Andromedae reside closer than this ice boundary.

Two possibilities can be considered for their formation. They may have formed outside the 4 AU ice–boundary. If so, some dynamical interaction with yet a fourth body would be required to drain orbital energy from the three observed Jupiter–mass companions to bring them closer to the star. Plausible candidates for the fourth body are a giant planet, a passing star, or the protoplanetary disk. Detailed models are required to determine the physical plausibility of these three candidates.

Alternatively, the three Jupiter–mass companions may have formed within 4 AU. If so, it is tempting to wonder if they formed *in situ*. Typical models of protoplanetary disks do not contain enough mass at 0.05 AU within a Hill sphere (tidal reach) of a Jupiter–mass planet. Thus it is difficult to explain *in situ* formation for the inner–most companion, unless either the surface mass density of the disk is higher than expected at 0.05 AU or the gas drains onto the planet from the outskirts of the disk.

The Lick Observatory team gratefully acknowledges the help of the Lick Observatory staff, including Tony Misch, Wayne Earthman, Keith Baker and John Morey. Lick observations have been carried out by Eric Williams and Chris McCarthy, who also contributed to software development. Steve Saar, Kevin Apps, and Greg Laughlin have provided useful advice and guidance. The Lick planet search team acknowledges support by NASA grant NAGW-3182 and NSF grant AST95-20443 (to GWM), and by Sun Microsystems. Lick time has been provided by the consideration of the Univeristy of California Telescope assignment committee. The AFOE team gratefully acknowledges the support of the Whipple Observatory staff, including Perry Berlind, Mike Calkins, Ted Groner, Robert Hutchins, Jim Peters, and Wayne Peters; and Tedd Russ at HAO. The AFOE group also acknowledges support from NASA grant NAG5–75005 and from the Smithsonian Institution Scholarly Studies program.

REFERENCES

Artymowicz, P. 1993, ApJ, 419, 166

Baliunas, S. L., et al. 1995, ApJ, 438, 269

Baliunas, S. L., Henry, G. W., Donahue, R. A., Fekel, F. C., & Soon, W. L. 1997, ApJ, 474, L119

Black, D. C. & Scargle, J. D. 1982, ApJ, 263, 854

Boss, A. P. 1995, Science, 267, 360

Brown, T. M., Noyes, R. W., Nisenson, P., Korzennik, S., Horner, S. D. 1994, PASP, 106, 1285

Brown, T. M., Kotak, R., Horner, S. D., Kennelly, E. J., Korzennik, S., Nisenson, P., & Noyes, R. W. 1998a, ApJ, 494, L85

Brown, T. M., Kotak, R., Horner, S. D., Kennelly, E. J., Korzennik, S., Nisenson, P., & Noyes, R. W. 1998b, ApJ Supp, 117, 563

Burrows, A., Marley, M., Hubbard, W. B., Sudarsky, D., Sharp, C., Lunine, J. I., Guillot, T., Saumon, D., & Freedman, R. 1998. In Proceedings of The Tenth Cambridge Workshop on Cool Stars, Stellar Systems and the Sun, Ed. R. A. Donahue and J. A. Bookbinder, ASP Conf. Ser. 154, p.27

Butler, R. P., Marcy, G. W., Williams, E., McCarthy, C., Dosanjh, P., & Vogt, S. S. 1996, PASP, 108, 500

Butler, R. P., Marcy, G. W., Williams, E., Hauser, H., & Shirts, P. 1997, ApJ, 474, L115

Cochran, W. D., Hatzes, A. P., Butler, R. P., & Marcy, G. M. 1997, ApJ, 483, 457

de la Fuente Marcos, C. & de la Fuente Marcos, R. 1997, A&A, 326, L21

Duquennoy, A. & Mayor, M. 1991, A&A, 248, 485

Edvardsson, B., Anderson, J., Gustafsson, B., Lambert, D. L., Nissen, P. E., & Tomkin, J. 1993, A&A, 275, 101

Fischer, D. A., Marcy, G. W., Butler, R. P., Vogt, S. S., & Apps, K. A. 1999, PASP, 111, 50

Ford, E. B., Rasio, F. A., & Sills, A. 1998, preprint, submitted to ApJ.

Fuhrmann,K., Pfeiffer,M.J., Bernkopf,J. 1998, AA, 336,942

Gladman, B. 1993, Icarus, 106, 247

Goldreich, P., Tremaine, S. 1980, ApJ, 241, 425

Gonzalez, G. 1997, MNRAS, 285, 403

Gray, D. F. 1992, The Observation and Analysis of Stellar Photospheres, Cambridge University Press.

Gray, D. F. 1997, Nature, 385, 795

Gray, D. F. 1998, Nature, 391, 153

Guillot,T., Burrows,A., Hubbard,W.B., Lunine,J.I., Saumon,D. 1996, ApJL, 459, L35

Hatzes, A. P. & Cochran, W. D. 1998, ApJ, 502, 944

Hatzes, A. P., Cochran, W. D., & Bakker, E. J. 1998, Nature, 391, 154

Hoffleit, D. 1982, The Bright Star Catalogue, (Yale University Observatory)

Holman, M., Touma, J. & Tremaine, S. 1997, Nature, 386, 254

Larson, A. M., Irwin,A. W., Yang, S. L. S., Goodenough, C., Walker,G. A. H., Walker,A. R., Bohlander,D. A. 1993, PASP, 105, 332

Laughlin, G. & Adams, F. C. 1998, ApJ, 508, L171

Levison, H. A., Lissauer J. J., & Duncan, M. J. 1998, AJ, 116, 1998

Lin, D. N. C. & Papaloizou, J. C. B. 1986, ApJ, 309, 846

Lin, D. N. C., Bodenheimer, P., & Richardson, D. C. 1996, Nature, 380, 606

Lissauer JJ. 1995. Icarus, 114, 217

Marcy, G. W. & Butler, R. P. 1998, ARAA, 36, 57.

Marcy, G. W., Butler, R. P., Williams, E., Bildsten, L., Graham, J. R., Ghez, A., & Jernigan, G. 1997, ApJ, 481, 926

Marcy, G. W. & Butler, R. P. 1992, PASP, 104, 270.

Mayor, M., Beuzit, J. L., Mariotti, J. M., Naef, D., Perrier, C., Queloz, D., & Sivan, J. P. 1998, ASP Conf. Ser. (in press), IAU Colloq. 170: Precise Stellar Radial Velocities, ed. J.B. Hearnshaw & C.D. Scarfe, (San Francisco: ASP)

Mazeh, T., Krymolowski, Y. & Rosenfeld, G. 1997, ApJ, 477, L103

McMillan, R. S., Moore, T. L., Perry, M. L., & Smith P. H. 1993, ApJ, 403, 801

Morbey, C. L. & Griffin, R. F. 1987, ApJ, 317, 343

Noyes, R. W., Jha, S., Korzennik, S. G., Krockenberger, M., Nisenson, P., Brown, T. M., Kennelly, E. J., & Horner, S. D. 1997, ApJ, 483, L111

Perryman, M. A. C., et al. 1997, The Hipparcos Catalog. A&A, 323, L49.

Queloz, D. & Henry, G. W. 1998, in preparation, to be submitted to ApJ.

Rasio, F. A., & Ford, E. B. 1996, Science, 274, 954

Saar, S. H., Butler, R. P., & Marcy, G. W. 1998, ApJ, 403, L153.

Saar, S. H., & Donahue, R. A. 1997, ApJ, 485, 319.

Shine,R.A. & Linsky,J.L. 1972, Solar Physics, 25, 357

Shirts, P. & Marcy, G. W. 1999, preprint in preparation.

Trilling D., Benz W., Guillot T., Lunine J. I., Hubbard W. B., Burrows A., 1998, submitted to ApJ

Vogt, S. S. 1987, PASP, , 99, 1214

Walker, G. A. H., Walker, A. R., Irwin, A. W., Larson, A. M., Yang, S. L. S., Richardson, D. C. 1995, Icarus, 116, 359

Ward, W. R. 1997, ApJ, 482, L211

Weidenschilling, S. J. & Marzari, F. 1996, Nature, 384, 619

This preprint was prepared with the AAS LATEX macros v4.0.

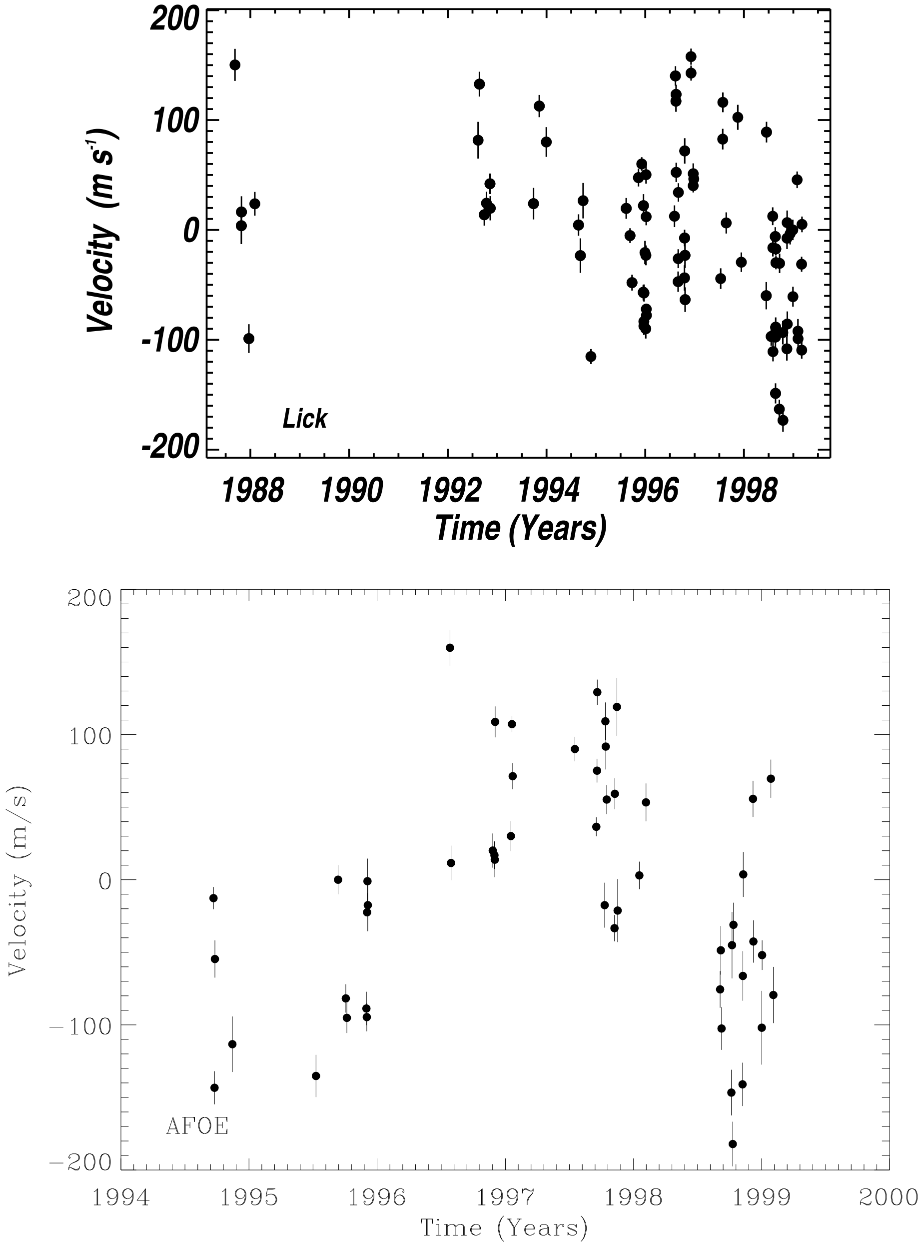

Fig. 1.— Observed Doppler measurements for υ Andromedae from a) Lick Observatory, b) AFOE. The velocity zero-point is arbitrary and independent in each set of data.

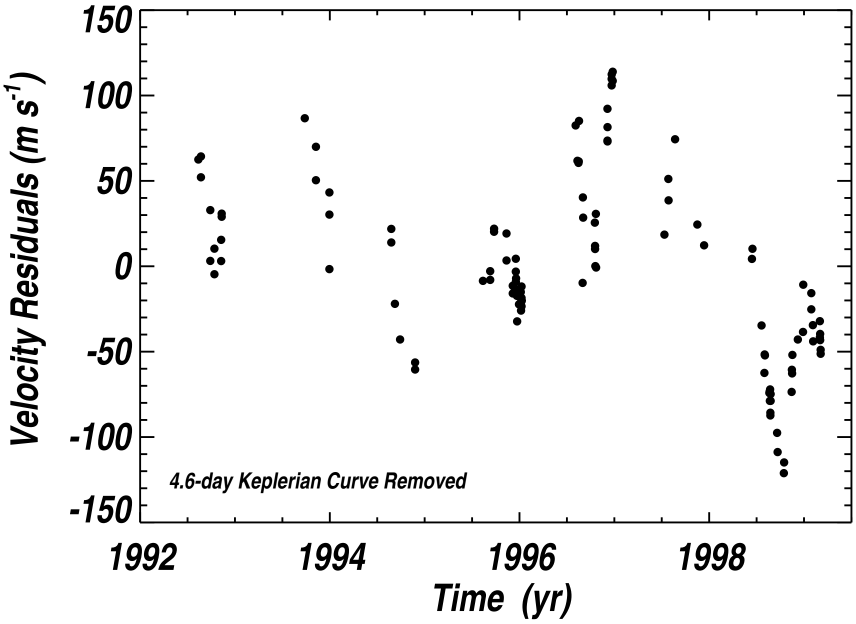

Fig. 2.— Lick Observatory residual velocities for υ Andromedae after removal of the Keplerian wobble caused by the inner companion, using best–fit orbital parameters of P=4.6171 d and K=75 m s^{-1}. The residual velocities are not random. Two time scales are apparent at 3 yr and ∼0.7yr, the latter especially apparent from 1998.5 to 1999.2 (bottom right).

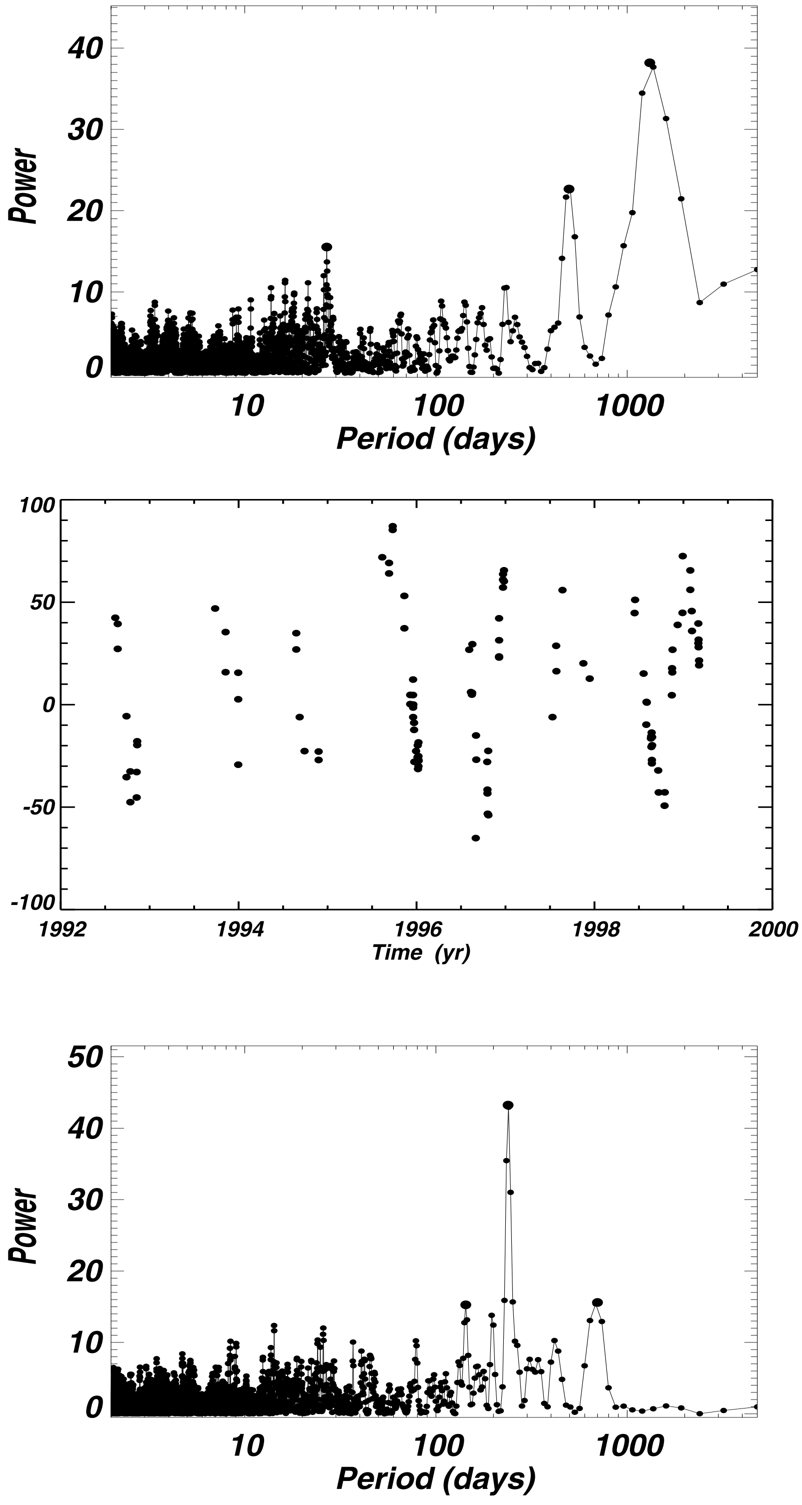

Fig. 3.— a) Periodogram of the Lick velocity residuals, after removal of the 4.6-day period companion. The peak power at 1200 d corresponds to the 3-yr time scale that was visually apparent in the residuals in Figure 2. b) Residual velocities for Lick observations, after subtracting both Keplerian velocity curves with periods of 4.6 d and 1269-d. Best-fit parameters were used in constructing the Keplerian for the long-period companion, P=1269 d, K= 69.5 m s^{-1}, and e=0.36. These residuals are still not random, and carry a χ^2 of 4, indicating that the model containing two companions remains inadequate. The time scale of $\sim$0.7 yr remains apparent, as in Figure 2. c) Periodogram of the residuals from part b. Peak power is found at a period of $\sim$230 d, indicating a statistically-significant third periodicity.

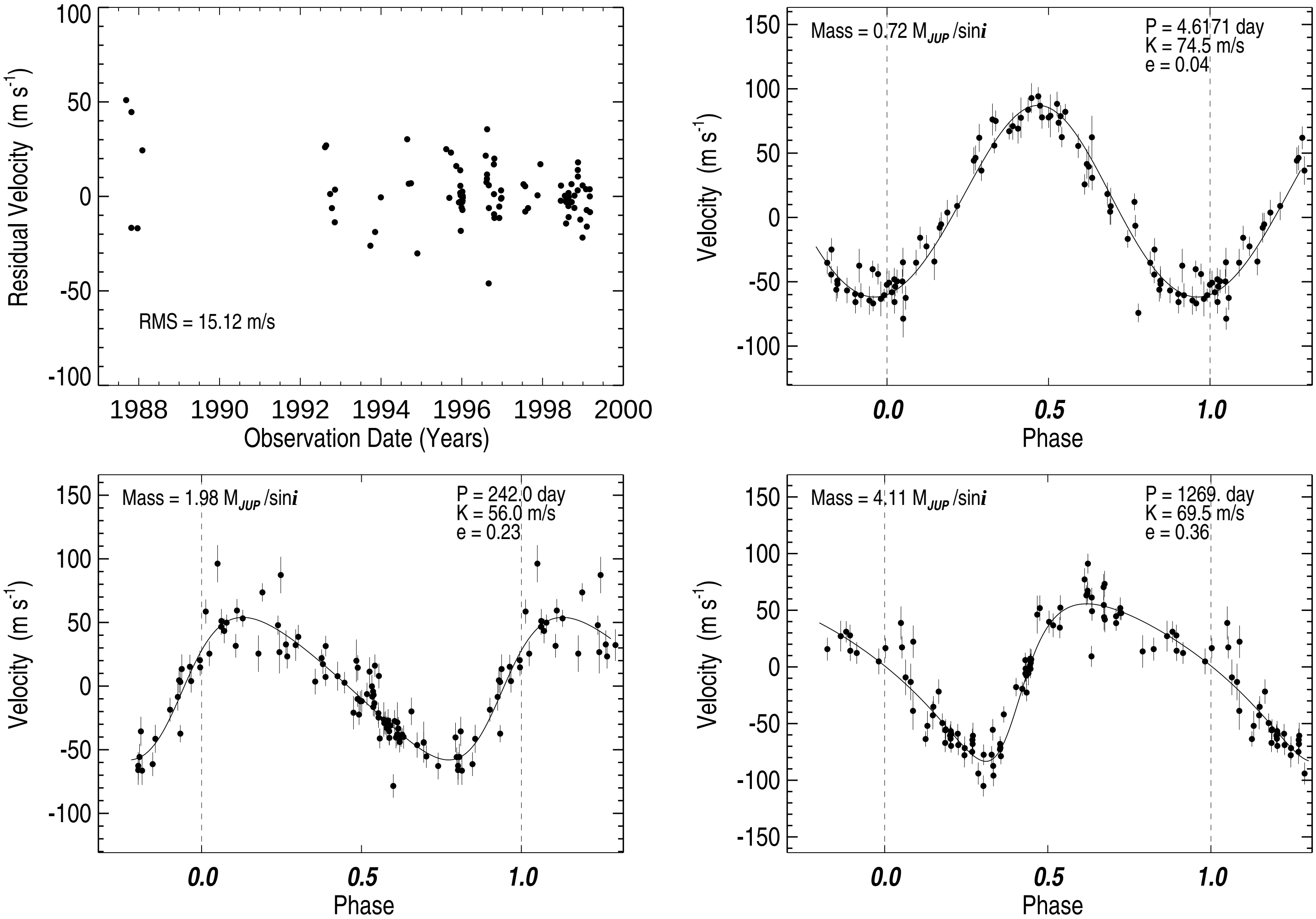

Fig. 4.— a) Residual velocities for Lick observations of υ Andromedae after removal of the Doppler velocity variations from all 3 companions (b,c,d). A periodogram search of these residuals does not show significant power at any additional frequencies. b) Residual velocities after the Doppler velocities attributed to companions c and d were subtracted from the observed velocities. The residual velocity variation due to the short-period companion b is plotted vs. orbital phase. c) Residual velocities after the Doppler velocities attributed to companions b and d were subtracted from the observed velocities. The residual velocity, plotted vs. orbital phase exhibits the 242 day periodicity of companion c. d) Residual velocities after the velocity variations from the inner two companions (b,c) were subtracted from the observed velocities and the residual velocities with a 1269 day periodicity are plotted vs. orbital phase. In all three phased velocity plots, the solid line is the Doppler velocity curve from the Keplerian orbital solution.

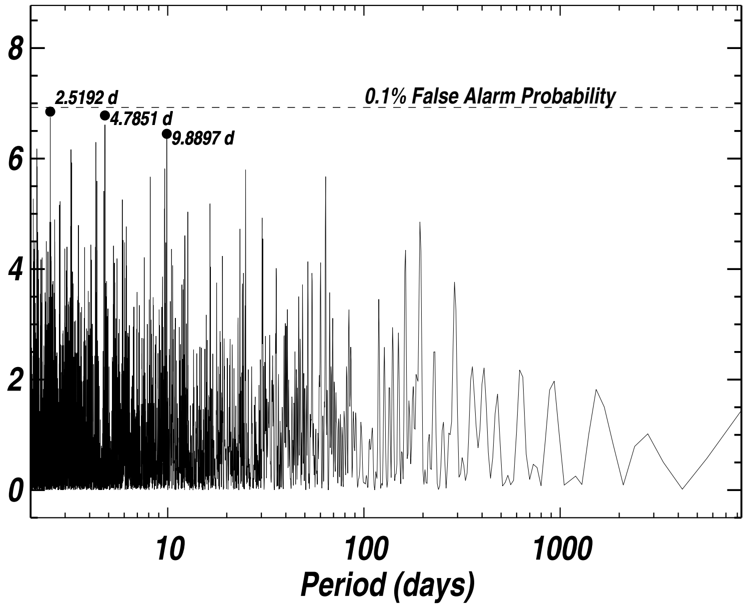

Fig. 5.— Periodogram of the Lick velocity residuals after subtracting Keplerian velocity curves for all three companions. The best fit parameters to the Lick data were used to construct the Keplerian curves. There are no additional peaks with significant power in the residuals.

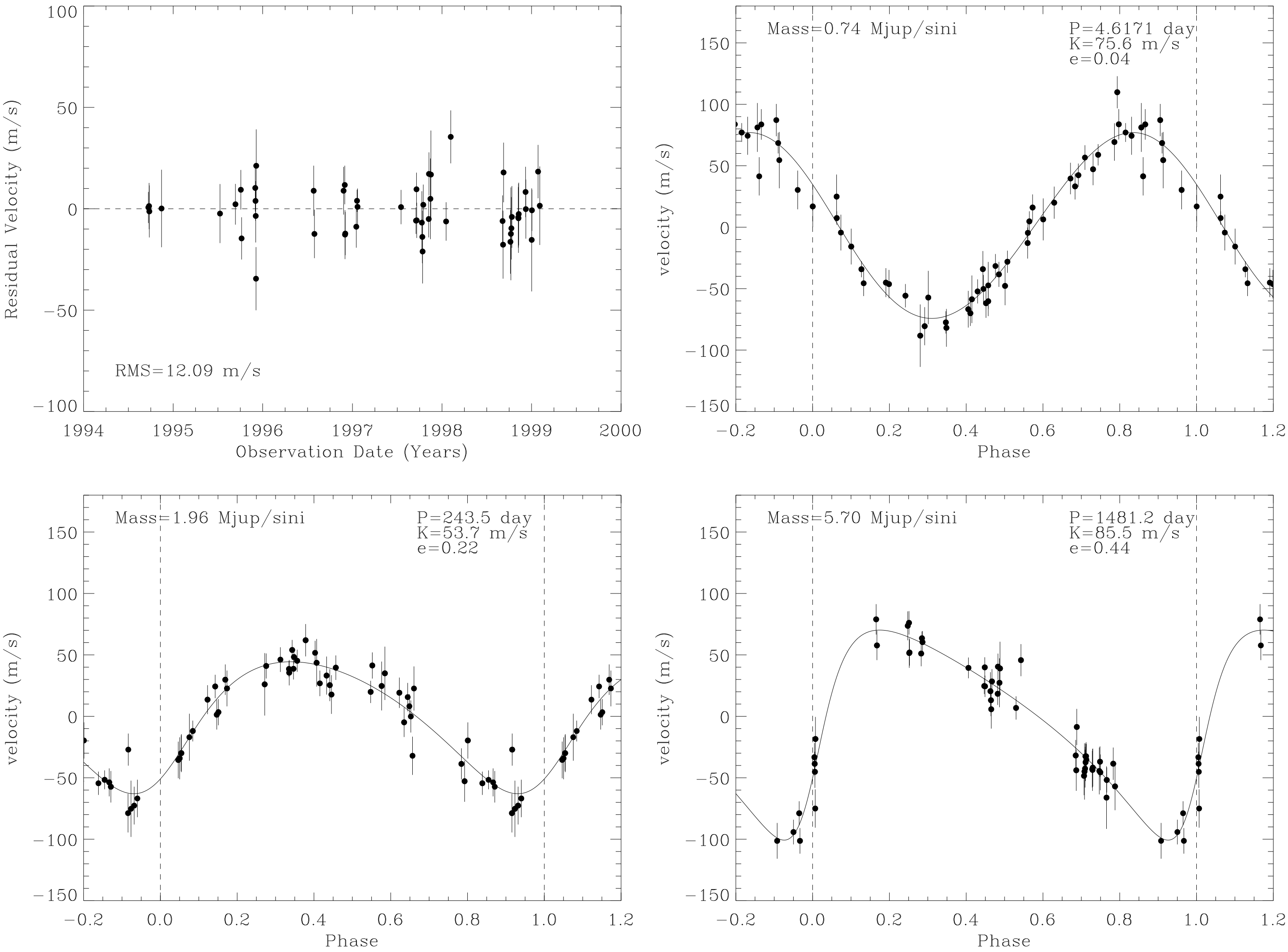

Fig. 6.— a) Residual velocities from AFOE observations of υ Andromedae, after removal of the Doppler velocity variations from all three companions according to the fits to the AFOE data alone (Table 3). b) Residual velocities after the fitted velocities attributed to companions c and d are subtracted from the observed data, plotted vs. orbital phase of companion b with period 4.617 d. c) Residual velocities after subtraction of the fitted velocities for companions b and d, plotted vs. orbital phase of companion c with period 244 d. d) Residual velocities after subtraction of the fitted velocities for companions b and c, plotted vs. orbital phase of companion d with period 1481 d.

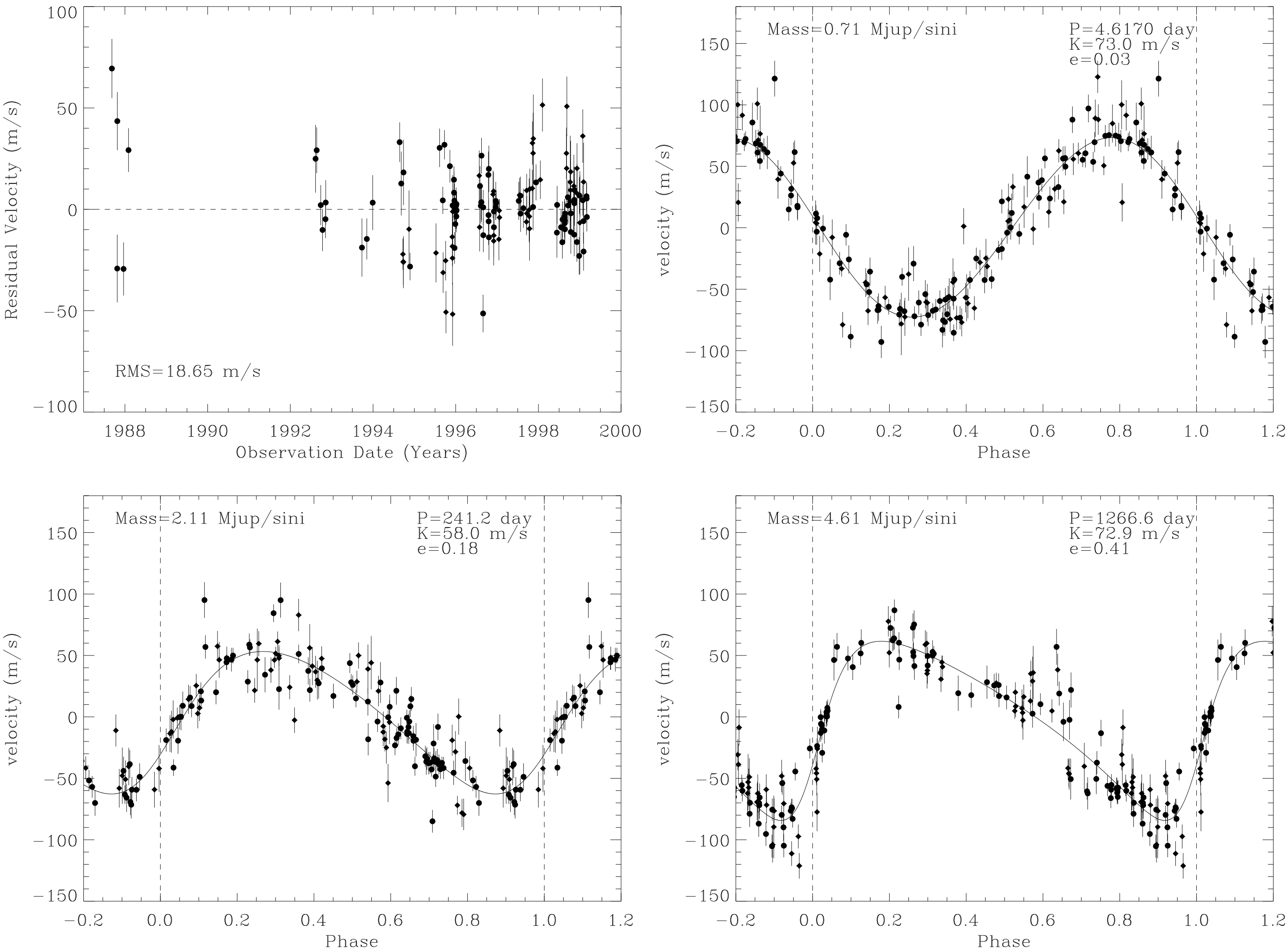

Fig. 7.— Velocities from the combined data sets from Lick and AFOE. Circles represent the Lick data and diamonds the AFOE data. a) Velocity residuals of the combined data to the fit that contains three companions. b) Residuals after the velocities attributed to companions c and d are subtracted from the combined velocities, plotted vs. orbital phase of companion b with period 4.617 d. c) Residuals after subtraction of the combined velocities for companions b and d, plotted vs. orbital phase of companion c with period 241 d. d) Residuals after subtraction of the combined velocities for companions b and c, plotted vs. orbital phase of companion d with period 1267 d.

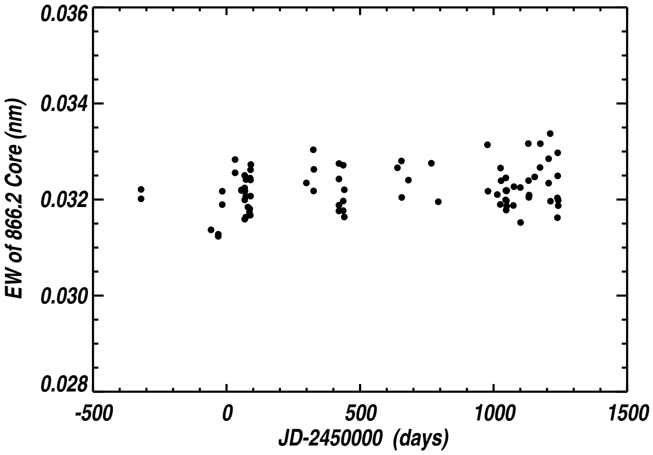

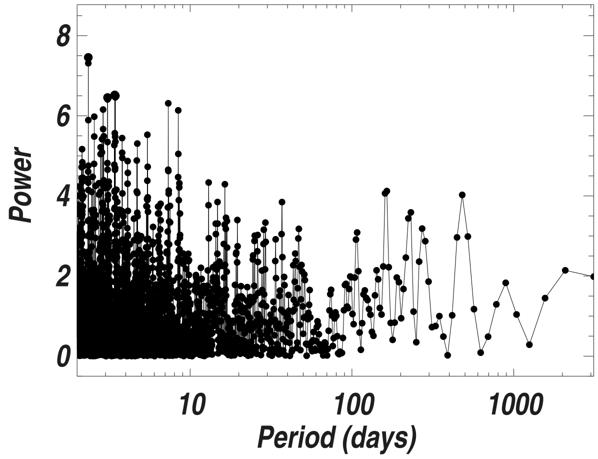

Fig. 8.— a) Equivalent Width of the chromospheric core of the CaII line at 866.2 nm vs time for υ Andromedae. The equivalent width measures the chromospheric "filling in" of the 0.07 nm core band. b) Periodogram of 8a, showing any periodicities in the chromospheric emission. No significant peak is found, but weak peaks at P = 200-300 warrant continued measurements.

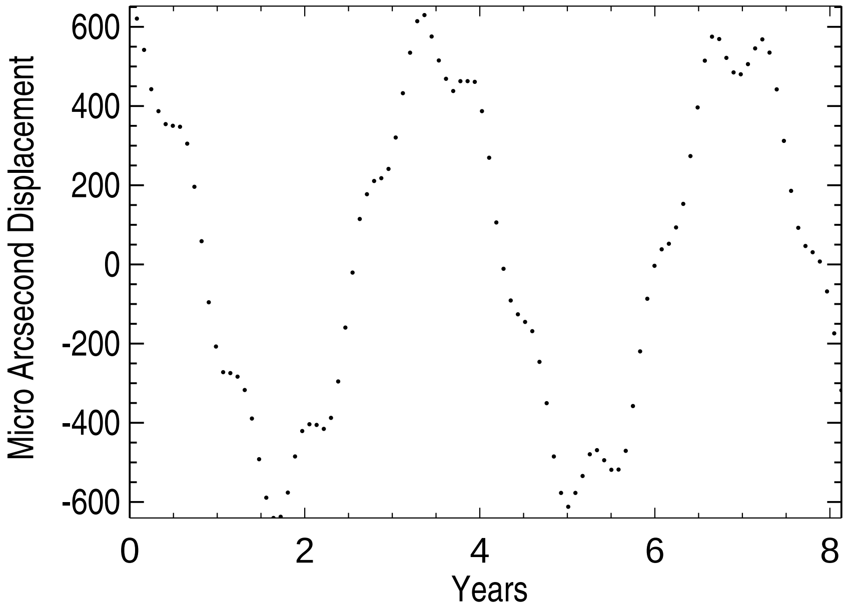

Fig. 9.— Expected astrometric signature of the υ Andromedae system. Gaussian noise of 4 μas RMS has been added to the calculated displacement to simulate the expected SIM measurement uncertainty. The low angular displacement of the star due to companion b renders this closest component undetectable by SIM. The c and d companions would exhibit displacements that should be detected by SIM.

Table 1. Lick Radial Velocities for HR 458

JD -2440000	RV m s^{-1}	σ_{VEL} m s^{-1}
7046.922	137.16	14.59
7093.759	-9.23	16.70
7094.762	3.30	14.32
7149.778	-111.99	13.11
7193.629	10.74	10.80
8845.965	68.60	16.70
8855.934	119.66	11.29
8891.935	0.77	9.89
8907.838	11.27	10.47
8933.828	28.96	9.35
8935.848	6.70	11.06
9255.855	10.86	14.34
9298.803	99.69	10.12
9350.706	66.99	13.54
9588.992	-8.59	9.78
9602.962	-36.44	15.74
9622.928	13.56	16.13
9680.753	-119.38	6.79
9942.008	15.45	9.49
9969.980	-9.32	6.70
9984.853	-52.14	7.23
10032.740	43.45	8.08
10056.842	55.90	6.18
10068.586	-60.85	6.58
10068.774	-61.18	7.24
10069.599	17.93	10.52
10072.603	-87.49	8.55
10072.724	-91.61	8.12
10073.652	-61.58	7.78
10080.782	-24.74	10.62
10086.739	-94.13	8.88
10087.689	-27.28	9.03
10088.741	46.13	8.16

Table 1—Continued

JD -2440000	RV m s^{-1}	σ_{VEL} m s^{-1}
10089.710	7.91	7.83
10090.646	-76.23	5.02
10091.663	-81.87	9.10
10299.008	8.32	9.88
10305.992	136.04	8.86
10310.001	113.06	9.69
10310.996	119.22	8.75
10311.984	48.23	8.78
10325.891	-51.27	9.27
10326.914	-30.32	8.60
10327.918	29.98	8.42
10372.958	-47.82	11.55
10373.839	-11.51	7.56
10374.884	67.76	11.59
10376.910	-27.30	11.48
10377.811	-67.62	11.22
10421.568	153.61	7.34
10421.756	138.62	6.85
10437.686	36.08	6.13
10437.870	47.01	9.44
10441.772	42.27	6.33
10640.983	-48.48	9.40
10655.995	78.50	9.42
10656.945	112.01	9.02
10681.982	2.21	9.65
10767.728	98.36	11.40
10793.716	-33.54	8.89
10977.996	-64.01	12.42
10979.992	84.87	9.40
11014.980	-101.16	8.42
11025.971	8.30	8.13
11026.954	-20.41	7.93
11028.007	-114.93	8.89

Table 1—Continued

JD -2440000	RV m s^{-1}	σ_{VEL} m s^{-1}
11045.019	-10.20	8.54
11046.007	-101.66	9.26
11046.985	-152.94	9.18
11047.957	-92.68	8.92
11048.930	-21.44	5.96
11049.916	-34.02	5.98
11074.914	-167.28	8.65
11076.903	-34.57	8.87
11100.904	-97.60	10.74
11101.878	-177.46	10.38
11130.855	-112.39	10.70
11131.799	-11.68	9.88
11132.721	2.49	11.04
11133.840	-89.83	11.51
11154.726	-7.62	9.74
11174.670	-4.14	9.32
11175.607	-64.92	9.05
11206.646	41.48	7.57
11212.674	-96.32	11.07
11213.666	-103.19	9.45
11239.635	-35.37	6.85
11240.646	-113.57	7.77
11242.635	0.90	7.14

Table 2. AFOE Radial Velocities for HR 458

JD -2440000	RV m s^{-1}	σ_{VEL} m s^{-1}
9617.921	-7.36	7.68
9620.828	-138.01	11.40
9621.875	-49.31	12.83
9671.674	-108.00	19.12
9909.990	-129.87	14.57
9972.946	5.33	10.05
9994.956	-76.46	9.76
9997.988	-89.85	10.42
10053.697	-83.41	11.56
10054.764	-89.32	9.82
10055.685	-17.12	13.08
10056.754	4.31	15.58
10057.685	-12.20	17.96
10291.933	165.16	12.38
10294.952	16.87	11.96
10413.793	25.42	11.78
10418.645	22.23	9.52
10419.641	19.14	12.09
10420.685	114.07	10.66
10465.597	35.39	10.35
10468.606	112.51	5.46
10470.658	76.66	9.03
10647.968	95.36	8.47
10708.991	41.79	6.55
10711.011	80.46	8.21
10711.838	134.52	8.69
10732.837	-12.21	15.49
10734.862	114.47	13.01
10735.928	97.05	15.76
10738.695	60.57	9.99
10760.795	-28.08	9.08
10761.838	64.52	10.65
10767.762	124.40	19.89

Table 2—Continued

JD -2440000	RV m s^{-1}	σ_{VEL} m s^{-1}
10769.817	-15.92	21.72
10831.645	8.29	9.49
10850.580	58.61	13.07
11061.888	-70.25	12.66
11063.921	-43.32	16.75
11065.967	-97.18	14.72
11093.936	-141.33	15.73
11095.838	-39.77	22.90
11097.848	-176.76	15.38
11099.868	-25.74	15.25
11125.812	-135.65	14.93
11126.714	-60.96	17.08
11127.776	8.97	15.47
11155.644	61.05	12.44
11156.725	-37.24	14.58
11180.641	-96.65	25.42
11181.587	-46.62	10.19
11206.611	74.93	13.17
11213.581	-74.08	19.37

Table 3. Orbital Parameters

Parameters	Lick data	AFOE data	Combined Lick/AFOE
Companion b			
P (d)	4.6171 ± 0.0001	4.6171 ± 0.0003	4.6170 ± 0.0003
T_{peri} (JD)	2450315.34 ± 0.7	2450001.99 ± 0.51	2450002.24 ± 3.1
e	0.042 ± 0.030	0.042 ± 0.033	0.034 ± 0.15
ω (deg)	16.0 ± 139	63.8 ± 40	83.0 ± 243
K_1 (m s^{-1})	74.5 ± 2.3	75.6 ± 2.3	73.0 ± 5
$a_1 \sin i$ (AU)	3.16×10^{-5}	3.21×10^{-5}	3.10×10^{-5}
a_b (AU)	0.059	0.059	0.059
$M_b \sin i$ (M_{JUP})	0.72	0.74	0.71
Companion c			
P (d)	242.0 ± 0.7	243.5 ± 1.0	241.2 ± 1.1
T_{peri} (JD)	2451131.24 ± 23.4	2450140.4 ± 8.3	2450154.9 ± 20.8
e	0.23 ± 0.06	0.22 ± 0.06	0.18 ± 0.11
ω (deg)	261.0 ± 47	219.2 ± 14	243.6 ± 33
K_1 (m s^{-1})	56.0 ± 2.5	53.7 ± 3.5	58.0 ± 7.9
$a_1 \sin i$ (AU)	0.0012	0.0012	0.0013
a_c (AU)	0.83	0.83	0.83
$M_c \sin i$ (M_{JUP})	1.98	1.96	2.11
Companion d			
P (d)	1269.0 ± 8.5	1481.2 ± 35	1266.6 ± 30
T_{peri} (JD)	2453813.46 ± 32.0	2450046.8 ± 16.1	2451308.7 ± 40.5
e	0.36 ± 0.05	0.44 ± 0.05	0.41 ± 0.11
ω (deg)	236.0 ± 14.6	245.9 ± 5.9	247.7 ± 17.0
K_1 (m s^{-1})	69.5 ± 2.1	85.5 ± 4.0	72.9 ± 7.1
$a_1 \sin i$ (AU)	0.0076	0.0105	0.0077
a_d (AU)	2.50	2.78	2.50
$M_d \sin i$ (M_{JUP})	4.11	5.70	4.61
N(obs)	89	52	141
RMS residuals (m s^{-1})	15.12	12.1	18.7